Energy Characterization and Optimization of New Heat Recovery Configurations in Hybrid PVT Systems

María Herrando[1], Ilaria Guarracino[2], Alejandro del Amo[3], Ignacio Zabalza[1], Christos N. Markides[2]

[1] Centre of Research for Energy Resources and Consumption (CIRCE), University of Zaragoza, Zaragoza, Spain

[2] Clean Energy Processes (CEP) Laboratory, Department of Chemical Engineering, Imperial College London, London (UK)

[3] EndeF Engineering, Zaragoza (Spain)

Abstract

The main goal of this research is to design and assess a new heat recovery (absorber-exchanger) configuration for a hybrid PVT solar panel with a geometry and from a material that maximises heat transfer while reducing weight and cost. To this end, firstly, potential configurations and materials for the absorber-exchanger unit that have the potential to meet the aforementioned aim are considered. The selected configurations (plus a benchmark reference case) are then applied to the same PVT panel in order to compare their performance. Once these configurations are defined in detail, they are modelled in 3-D finite-element and multiphysics (FEM and CFD) software, specifically COMSOL. The objectives are to: i) maximize the heat transfer performance of the different absorber-exchanger configurations, ii) obtain characteristic curves that describe the steady-state performance of the PVT panel in each case, and iii) compare the different alternatives with the reference case. The results show that a polymeric flat-box configuration is a promising alternative to commercial PVT panels, being able to achieve an improvement in the thermal performance of the PVT unit compared to the reference case (up to 5.1% higher optical efficiency and up to 48.7% lower heat loss coefficient), while also lowering the weight (up to 12%) and investment costs (up to 22%) of the PVT panel.

Keywords: *hybrid PVT panel, absorber-exchanger unit, heat transfer, energy efficiency, energy modelling*

1. Introduction

Currently, PV systems only use ~15% of the solar radiation, losing the remaining 85% as heat which, if recovered, could be used to heat a circulating fluid such as air or water. This has been the main motivation behind the development of hybrid PVT systems, which simultaneously generate electricity and a thermal output, and are considered a very promising technology for electricity and heat provision in buildings (Herrando et al., 2014). In particular, PVT-water (PVT-w) systems can increase the efficiency of PV panels by up to ~15% while generating hot water suitable to provide Domestic Hot Water (DHW) or space heating, so it is believed that this technology has an important potential in the residential sector, which accounts for 25% of the total electricity and 29% of the final energy consumption in the European Union (Antonanzas et al., 2015).

Previous research undertaken by the authors concluded that PVT-w systems can cover up to 50% of the total electricity demand and 35% to 50% of the DHW demand of a typical household located in London (the UK) (Guarracino et al., 2016c; Herrando et al., 2014), while completely covering the electricity demand and around 70% of the DHW demand if located in a household in Larnaca (Cyprus) (Guarracino et al., 2016a). Furthermore, as previous authors noted (Allan et al., 2015), the most desirable aspect of the PVT technology is the more efficient use of the roof space compared to stand-alone PV and solar collector systems.

Since their appearance, commercial PVT systems have been made available with increased in efficiency, making these panels an interesting option for integration in buildings. However, there are still very few companies worldwide that commercialise this type of PVT panel (Herrando and Markides, 2016) and most of the products available on the market do not have an optimised design for PVT applications. For this reason, the International Energy Agency (IEA), in its Task 35 for the development of PVT systems, insists on the need to optimise these systems from the manufacture and performance points of view, by developing projects that accelerate their economic viability to compete with current renewable energy technologies.

The main goal of this research is to develop an improved hybrid PVT module, with an optimal balance of energy efficiency, weight, cost, and ease of manufacturing. A number of alternative heat recovery (absorber-

doi:10.18086/eurosun.2016.08.22 Available at http://proceedings.ises.org

exchanger from now on) configurations are designed and compared with a reference case, all of them integrated in the same panel, for which a 3-D model is developed in COMSOL to model their energy performance, obtain their corresponding characteristic curve, and finally identify the design parameters which optimise the performance. The main focus is the study of a new absorber-exchanger configuration made of polymer and with a geometry that maximises heat transfer, while reducing the cost and weight of the PVT panel.

A detailed 3-D model of the PVT module is required to predict the non-uniform temperature distribution on the solar cells. In a previous work of Guarracino et al. (2016a), the 3-D PVT model showed a temperature gradient on the surface of a sheet-and-tube PVT module of ~10 °C during normal operating conditions, which led to a 5% drop in cell efficiency at the hot spots compared to cooler points, with a consequent loss in the PVT panel electrical performance. Therefore, the aim here is to achieve a uniformly cooled PVT module through the identification in the 3-D PVT model of the solar cells' hot spots and their elimination as far as possible.

In this work, a commercially available PVT sheet-and-tube collector (ECOMESH panel) model is implemented in COMSOL and validated with experimental results provided by the panel manufacturer, EndeF Engineering. COMSOL allows the investigation of more complex geometries which are not easy to model mathematically without a graphic tool, thus once the COMSOL model of the commercial PVT panel is validated, the model can be used with confidence to evaluate the temperature distribution and the thermal performance of different geometries of absorber-exchanger of the PVT unit. Specifically, a flat-box configuration is investigated in the present paper, and other more complex geometries will be considered in future work.

2. Hybrid PVT panel selection

In the last decades, significant research has been undertaken giving rise to a large number of PVT water (PVT-w) system configurations, both in terms of material and geometry. Copper is the most widespread material used for several reasons, such as its high thermal conductivity. Among all the absorber-exchanger configurations found in literature, parallel tubes (sheet-and-tube) is the most common (Chow, 2003; Chow et al., 2007; Herrando et al., 2014; Kalogirou, 2001; Tripanagnostopoulos et al., 2005; Zondag et al., 2003), also used in various commercially available PVT panels. Regarding the PVT panel cover, several configurations have been studied: uncovered, with one or two covers, with or without gap between the cover and the PV cells, as well as different filling gases: air, inert gases or vacuum. The authors decided to use as benchmark reference case a commercial copper parallel tubes PVT panel, ECOMESH (EndeF Engineering), with an innovative Transparent Insulating Cover (TIC), with which the thermal efficiency is significantly improved while maintaining the electricity generated (Antonanzas et al., 2015; del Amo et al., 2016).

On the other hand, other authors (Chow et al., 2006, 2007; He et al., 2006) have studied other PVT configurations, such as the flat-box structure made of extruded aluminium alloy, with the aim to improve the fin efficiency and bonding quality, and hence the heat transfer. Therefore, as a first alternative to the reference case, aluminium flax-box is considered in an attempt to reduce the weight and cost of the absorber-exchanger unit, while improving (or at least maintaining) the thermal efficiency of the panel.

However, the main innovation and focus of this work is the study of a new absorber-exchanger configuration made of polymer, as it is believed that some polymeric materials such Polycarbonate (PC) or Polyamide (PA) have several properties that make them an interesting option for PVT collectors, such as (Cristofari et al., 2009): low density, mechanical strength, no special surface treatment required, no corrosion, ease of manufacturing at mass production as there are fewer components to assemble, and lower production cost because the material is generally cheaper and the manufacturing time is reduced. Nonetheless, there are also some disadvantages, such as the low thermal conductivity, large thermal expansion and limited service temperature. Specifically, the ideal polymer for this application should have the following properties: UV protected, high thermal conductivity, water-resistant and glycol-resistant, good thermal range of utilization (-10/+150°C), a good mechanical strength and be chemically stable (Cristofari et al., 2002, 2009, 2012). Bearing in mind this, two types of polymer are considered in the present research: Polycarbonate (PC), as suggested by previous authors (Cristofari et al., 2002, 2012; Huang et al., 2001) and Polyamide (PA) without and with additives to improve its thermal conductivity (Ghaffari Mosanenzadeh et al., 2015). Regarding the geometry, flat-box structure is the most common configuration studied with different channel dimensions. Examples are Huang et al. (2001) who considered channels of 6×4 mm (W×H), or Cristofari et al. (2009) who studied bigger channels of 10×10 mm (W×H), based on the results of parametric analysis undertaken in previous research (Cristofari et al., 2002), which concluded that the highest thermal energy gain is achieved with a fluid layer thickness of 1 mm. The study also concluded that, to collect more than 90% of this energy, the collector should have a fluid layer thickness smaller than 10 mm.

Although some of the absorber-exchanger configurations proposed in this work were studied previously, this research is innovative in the following aspects: i) these configurations were not implemented in high efficiency PVT units such as the one proposed (ECOMESH panel), but in PVT panels uncovered or covered with an air gap; ii) none of the studies found proposed a detailed study through 3-D FEM and CFD software of the absorber-exchanger alternatives considered in this work, integrated in the same PVT panel; iii) so far it has not been found any work that studied Polyamide with additives for the absorber-exchanger unit.

3. Methodology

Firstly, each absorber-exchanger configuration is defined in detail (geometry, technical specifications, etc.), integrated in the same PVT panel, and the energy balance of the PVT unit considering radiation, convection and conduction heat exchanges among the layers is developed. The reference PVT unit is then graphically implemented in COMSOL, together with its parameters and physics associated. Thanks to the symmetry of this sheet-and-tube geometry, only one riser tube of the PVT unit is implemented, significantly lowering the computation time and computational resources required by the 3-D model. The performance curve obtained is then compared with the empirical results provided by the PVT panel manufacturer (EndeF Engineering). Once the detailed 3-D model is validated, the different absorber-exchanger configurations are modelled to obtain the characteristic curve that describes the steady-state performance of the PVT panel in each case, i.e., the value of the optical efficiency (η_o) and linear and quadratic heat loss coefficients (a_1 and a_2). Finally, a simple cost analysis is undertaken to evaluate the different configurations studied from a cost perspective.

3.1 PVT panel modelling

The two main components of the PVT unit are the PV module and the rest of the solar collector, which can be further divided into the glazing, the thermal absorber and the riser water tubes (referred to, in the present work, as the absorber-exchanger or heat recovery unit) and the insulation layer (see Figure 1). Similarly to previous work by the authors (Herrando et al., 2014) and other PVT modelling attempts (Notton et al., 2005; Zondag et al., 2003), energy balances were written in order to evaluate the heat fluxes and temperatures throughout the unit. The equations were applied separately to each layer of the unit, instead of using global equations to find the average absorber plate temperature and energy flows (Kalogirou, 2004; Zondag et al., 2002). This allowed an estimation of the average temperatures of all the separate unit layers. Figure 1 shows the main heat transfer mechanisms of the PVT unit as well as the section with the different layers considered in the present work.

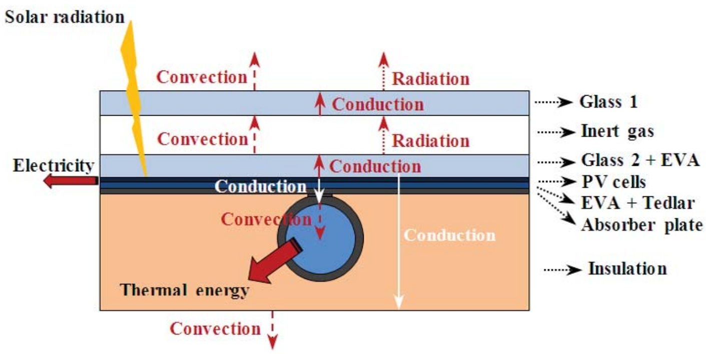

Fig. 1. PVT collector cross-section.

The PVT model was developed under the following main assumptions: i) Solar radiation is absorbed only by the collector (Agarwal and Garg, 1994); ii) the fraction of solar irradiance that is not converted into electricity in the PV cells and is not lost to the environment, is transmitted and absorbed in the absorber plate (Chow, 2003; Cristofari et al., 2009; Zondag et al., 2002, 2003), where most of it heats the water flowing through the collector and the rest is lost as heat (Agarwal and Garg, 1994); iii) the ambient temperature is considered uniform around the module (Cristofari et al., 2009; Notton et al., 2005) and heat transfer (losses) at the sides of the PVT collector are negligible (Notton et al., 2005), iv) the heat capacities of the PVT panel components (PV cells, Tedlar and insulation) are negligible compared to the heat capacity of water (Tiwari and Sodha, 2006); v) the water mass flow-rate is divided equally among all tubes of the collector (Bhattarai et al., 2012; Cristofari et al., 2009), the water flow-rate within the collector tubes is uniform and heat is transferred to the tubes by forced convection; and vi) radiative thermal exchanges between the sides of the solar collectors' channels are neglected (Chow, 2003; Cristofari et al., 2009; Sandnes and Rekstad, 2002; Zondag et al., 2002). The model was run under steady state conditions (Tiwari and Sodha, 2006; Zondag et al., 2003).

To compare the performance of the different absorber-exchanger configurations studied, the thermal efficiency of the PVT unit is calculated, following both the ASHRAE method (ASHRAE Standard, 2013) and the ISO method (ISO, 2013) for the performance testing of solar thermal collectors, as there is currently no standard method to assess the performance of a PVT collector (Allan et al., 2015).

The former is used to determine the heat removal factor (F_R) and the overall heat loss coefficient (U_L) of the PVT collector (Allan et al., 2015), by measuring or calculating (as in this case) the thermal efficiency of the collector at different inlet temperatures in steady state conditions (Antonanzas et al., 2015; Collins and Zondag, 2009; Sandnes and Rekstad, 2002; Vokas et al., 2006),

$$\eta_{th} = \frac{q_u}{G_i} = F_R(\alpha\tau)_{PV} - F_R U_L \frac{T_{in}-T_a}{G_i} \; ; \qquad \text{(Eq. 1)}$$

where η_{th} is the thermal efficiency of the PVT unit, q_u is the useful thermal energy extracted (W/m^2), G_i is the Incident irradiance (W/m^2), $(\alpha\tau)_{PV}$ is the combined transmission-absorption coefficient, T_{in} is the inlet water temperature and T_a is the ambient temperature.

Alternatively, in the ISO method, the PVT collector is also tested under steady state conditions but in this case the difference between the mean fluid temperature (T_{fm}) and the ambient temperature (T_a) is considered (Allan et al., 2015; Antonanzas et al., 2015; del Amo et al., 2016),

$$\eta_{th} = \frac{q_u}{G_i} = \eta_o - a_1 \frac{T_{fm}-T_a}{G_i} - a_2 G_i \left(\frac{T_{fm}-T_a}{G_i}\right)^2 \; ; \qquad \text{(Eq. 2)}$$

with $$T_r = \frac{T_{fm}-T_a}{G_i} \; ; \qquad \text{(Eq. 3)}$$

where η_o is the optical efficiency, a_1 is the heat loss coefficient which accounts for the linear heat loss variation, a_2 is the temperature dependence of the heat loss coefficient which accounts for the quadratic heat loss variation, T_{fm} is the mean fluid temperature and T_r is the reduced temperature.

One of the main limitations of detailed CFD-FEM 3-D simulations is the significant amount of both time and computational resources required, especially in problems involving multiple processes, e.g. thermal, fluid flow, etc. This is the case of hybrid PVT panels, where heat transfer and fluid-dynamic equations should be solved simultaneously. Furthermore, surface-to-surface radiation should also be considered to properly model covered PVT units, which adds an extra complexity to the model. Consequently, to lighten the problem without simplifying the physics (which would reduce the accuracy of the 3-D model), some simplifications are required. In the configurations studied in the present research, both the reference case (parallel riser tubes) and flat-box collectors have in common that all the riser pipes behave likewise, as the water mass flow-rate is divided equally among all tubes of the collector (Bhattarai et al., 2012; Cristofari et al., 2009), therefore symmetry can be applied to solve this problem. As consequence, only one pipe was implemented in COMSOL, applying symmetry boundary conditions on both sides of the model. However, even though the 1-pipe 3-D model worked for an uncovered PVT collector, when the Transparent Insulating Cover (TIC) was implemented, together with the physics involved (heat transfer in fluids in the gap and surface-to-surface radiation between PV glass and glass cover), the problem became too heavy to compute. Consequently, an additional symmetry was applied, considering half of the pipe with its corresponding half fin width (see Figure 2). To ensure the validity of this assumption, the results obtained in COMSOL for half pipe were validated with those of an entire pipe for the uncovered PVT panel.

Fig. 2. (Left) Cross section of a pipe and its fin and (right) half a pipe modelled in COMSOL Multiphysics

In the case of the flat-box structure, the geometry is simpler so it was possible to model a whole channel (20×10 mm, 40×10 mm), or two in the case of smaller dimensions (10×10 mm, 6×4 mm and 3×2 mm).

Examples of the type of results obtained from the COMSOL simulations are presented in Figure 3, where it is possible to observe on the left the PV layer temperature distribution and on the right 10 slices at different collector lengths of the temperature profile of the PVT layers throughout half of a pipe's fin, for the reference case. The results obtained for the reference PVT unit in the COMSOL model where validated with the experimental performance curve provided by the PVT panel manufacturer (EndeF Engineering).

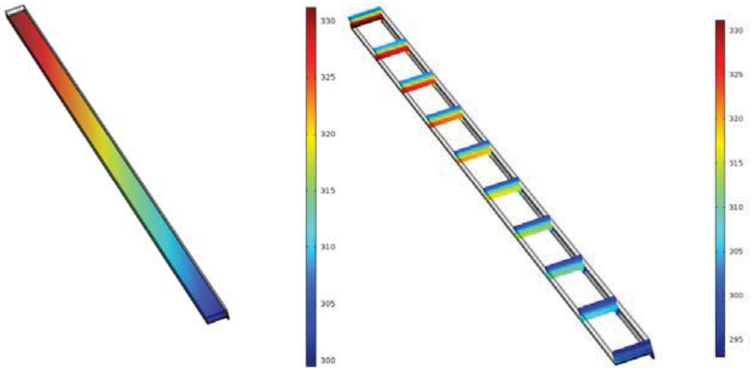

Fig. 3. (Left) PV layer temperature and (right) slices of the temperature profile in the different layers.

3.2 PVT unit parameters

The PVT unit taken as the reference case and modelled in this paper is the commercially available ECOMESH panel (EndeF Engineering), which consists of (from top to bottom): a Transparent Insulating Cover (TIC) comprising a transparent cover (glass) and an insulating gas (del Amo et al., 2016), a poly-crystalline (pc-Si) PV module, an EVA encapsulating film, an absorber-exchanger which transforms the solar radiation to heat and transfers it to the collector fluid (heat recovery unit), and a layer of insulation material at the bottom (see Figure 1). The absorber-exchanger unit consists of a sheet-and-tube heat exchanger in which water flows in (nine) copper parallel pipes (Antonanzas et al., 2015). The main PVT panel features are shown in Table 1. In order compare the different absorber-exchanger configurations studied in the present research, all the PVT parameters of the different layers were kept constant (panel dimensions, cover layers, PV cell, etc.), varying only the absorber-exchanger unit.

Tab. 1. Technical specifications of the PVT unit modelled (single module) (ECOMESH Panel) (EndeF Engineering)

Nominal power	240	W_p
Total gross area	1.64	m^2
Total aperture area	1.55	m^2
Recommended flow-rate range (nominal)	10-50 (30)	L/h
Reference PV module efficiency	14.7	%
Temperature coefficient of cell power (β_0)	-0.45	%/K
Normal Operating Cell Temperature (NOCT)	47	°C
Type of solar cell	Poly-crystalline (pc-Si)	

Tab. 2. Physical properties of the different polymeric materials considered

Properties	**PC***	**PA**	**PA90-15+**	**PA30-33+**	**PA ideal$**
hBN load	-	-	15 vol.%	33.3 vol.%	Max.
Density (ρ) (kg/m^3)	1,180	1,140	1,170	1,390	1,390
Thermal Conductivity (k) (W/(m·K))	0.775	0.26	1.2	3.6	30
Heat capacity (c_p) (J/(kg·K))	1,200	1,700†	1,700†	1,700†	1,700†

**(Cristofari et al., 2009, 2002); +(Ghaffari Mosanenzadeh et al., 2015);*

†The same heat capacity is considered for all Polyamides (PAs) as the addition of hBN does not significantly influence this physical property and its effect on the absorber-exchanger performance (within this order of magnitude) is negligible.

$An hypothetical polymer with a high thermal conductivity (30 W/(m·K)) is considered to study to which extent it is possible to improve the thermal performance of the absorber-exchanger unit with additives.

As alternative to the reference case, flat-box structure was considered. First of all, aluminium alloy was studied with two different channel dimensions, 20×10 mm (W×H) as suggested by several authors (Chow et al., 2006, 2007; He et al., 2006), and 10×10 mm (W×H), both with wall thickness of 2 mm. The properties of the aluminium alloy considered as those provided by Chow et al. (2006) (c_p = 903 J/(kg·K), ρ = 2702 kg/m^3, k = 237 W/(m·K)). Regarding polymeric materials for the absorber-exchanger unit, two main types of polymers were considered: Polycarbonate (PC) and Polyamide (PA), studying also some variations of the latter with different loadings of hexagonal Boron Nitride (hBN) particles (additive) (Ghaffari Mosanenzadeh et al., 2015). Table 2 summarizes the physical properties of different polymers considered.

Table 3 summarises all the geometric absorber-exchanger configurations considered in the present research.

Tab. 3. Summary of the absorber-exchanger configurations studied

<table>
<tr><th>Copper</th><th>Aluminium</th><th colspan="3">Polymer</th></tr>
<tr><td>3×2 mm
10×10 mm</td><td>10×10 mm
20×10 mm</td><td>3×2 mm
• PC
• PA30-33
6×4 mm
• PC
• PA30-33</td><td>10×10 mm
• PC
• PA
• PA90-15
• PA30-33
• PA ideal</td><td>20×10 mm
• PA
• PA30-33
40×10 mm
• PA
• PA30-33</td></tr>
</table>

All the PVT configurations detailed in Table 3 as well as the reference case are studied at steady state with the same initial conditions, detailed in Table 4. It should be noted that, even though according to the PVT manufacturer of the reference case the nominal flow-rate for the sheet-and-tube configuration is 0.0083 kg/s (30 L/h), the same collector flow-rate than for the flat-box configurations has been considered in this study to compare the alternatives under the same operating conditions.

Tab. 4. Initial conditions and other important constant system parameters

G_i	Incident solar irradiance	1000	W/m^2
T_a	Ambient temperature	25	°C
v_w	Wind velocity	1	m/s
T_{in}	Mains water temperature	20.2	°C
$\dot{m}_c$	Collector flow-rate	0.00533†	kg/s

†*Optimum flow-rate for the 10×10 mm flat-box configuration according to Cristofari et al. (2002, 2009)*

To complete the technical assessment, a simple cost analysis was undertaken in which the investment cost of each configuration was estimated, and the electricity and heat generation were converted to the same unit (€/h per PVT panel), so as they can be added up. To this intend, the actual electricity and natural gas price (€/kWh) in Spain were considered (see Table 5).

Tab. 5. Cost factors for the economic analysis

Cost analysis		Reference
Natural gas price	€/kWh	0.0508
Electricity price	€/kWh	0.14
Polymer cost	€/kg	2.3-3*
Additive (hBN) cost	€/kg	150
Aluminium 20×10 mm flat box cost	€/m	2.33
Ratio copper/aluminium cost	-	1.27
Extrusion production cost	€/m	2

**Price varies slightly between this range for PA, PA30, PA90 and PC*

The aim of the economical assessment is the estimation of the payback time (PBT) of the panels with Eq. (4) from the cost savings (€/h per PVT panel) and the investment costs (C_0). The payback time is estimated at constant weather conditions (Table 4) and represents a simple figure that can be used for comparison. The investment cost of the polymeric absorber-exchanger configuration is estimated from the cost of the raw polymeric material and the cost of adding the additive (hBN) where applicable, including also an estimation of the extrusion production cost. For the aluminium configurations, the price of off-the-shelf square channel tubes was considered, which was then extrapolated to the copper square channels considering the price ratio of both materials (Table 5).

$$PBT = \frac{C_0}{cost\ savings \cdot 24} \qquad \text{(Eq. 4)}$$

4. Results and discussion

4.1 Model Validation

The 3-D model developed in COMSOL was validated against a manufacturer's performance curve. In Figure 4 the thermal efficiency (η_{th}) is plotted against the reduced temperature (T_r). The 3-D model fits the experimental results with an average error of 19%, when the inlet water temperature is in the range 10-80°C, being the thermal performance overestimated with the largest deviation at high temperatures of operation. It should be noted that for inlet water temperatures lower than 30°C, the error is below 10%. This suggests that the heat losses are underestimated in the model. It should be noted that the model assumes a perfect thermal contact between the PV module and the rear copper sheet, and between the absorber and the pipe which are bonded, both assumption might explain the overestimation of the thermal performance. Guarracino et al. (2016b) found that that a poor thermal contact between the PV module and the thermal absorber, which resulted in an insulating air gap between the layers, reduces the thermal performance of the module up to 30%.

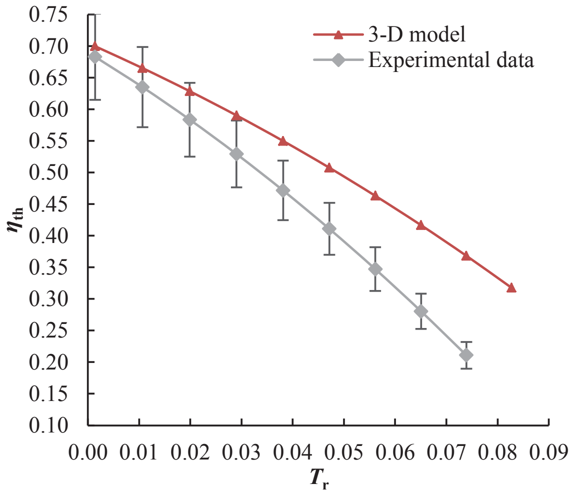

Fig. 4. Performance curves of the reference sheet-and-tube PVT unit for the COMSOL model, as well for the commercial ECOMESH panel (EndeF Engineering)

Regarding the heat transfer from the copper absorber to the tubes, a uniform bond made of copper and with fixed dimensions throughout the pipe is assumed, and both parameters influence the heat removal factor (F_R) and the overall heat loss coefficient (U_L) and hence the linear (a_1) and quadratic (a_2) heat loss coefficients. However, in reality depending on the bonding method (welding, ultrasounds, etc.) these will vary and hence the heat conduction will be achieved at lower or higher extent. Furthermore, lateral losses are not considered in the theoretical models. Finally, it should be noted that to obtain the experimental performance curve, the different experimental points are plotted in a T_r vs. η_{th} graph obtaining a cloud of points, and depending on which ones are selected to fit the curve, this might considerably vary .

4.2 Performance curve analysis

From the different PVT configurations studied and detailed in Table 3, first of all the effect of the material on the thermal efficiency of the PVT panel was assessed for the same channel dimensions (10×10 mm). First of all, it should be noted that, even though the thermal conductivity of all the polymers considered is lower than the one for copper, the heat transfer area between the polymer and the fluid is significantly larger than the sheet-and-tube configuration where the pipe is in contact with the copper only thought the bond. Furthermore, while for the sheet-and-tube collector the temperature on the PV cells reaches a maximum between two pipes, the temperature distribution on the PV surface is more uniform for the flat-box configuration, resulting in lower thermal losses (top thermal losses for the sheet-and-tube q_{top} = 138.06 W/m^2, while for the copper 10×10 flat box, q_{top} = 95.04 W/m^2). This is in agreement with the results found by previous studies that used polymeric flat-box absorber-exchanger units (Cristofari et al., 2009; Sandnes and Rekstad, 2002). As consequence, Figure 5 left shows that all flat-box configurations have better thermal performance than the sheet-and-tube collector, with a higher optical efficiency (η_o) (up to 4.3% better) and significantly lower heat loss coefficient (a_1) (up to 28.4% lower) in all the cases.

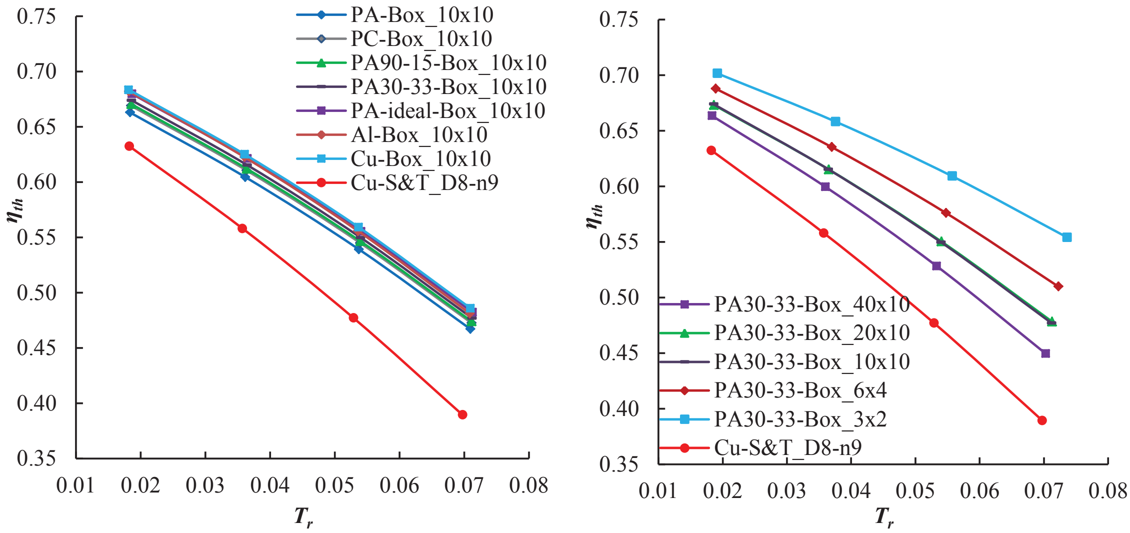

Fig. 5. Performance curves of the different PVT configurations studied for (left) same channel dimensions with different materials and (right) same material with different channel dimensions. In the legend, Cu-S&T_D8-n9, refers to 9 copper pipes of 8 mm external diameter.

It can also be observed that for the same channel dimensions, the difference in the performance curves between the best configuration (made of copper) and the worst one (made of Polyamide) is less than 5%, which implies that in this type of configuration the material selected is not determinant in the thermal performance of the PVT collector. This can be attributed to the small thickness of the polymeric absorber plate (1 mm).

On the other hand, Figure 5 right shows that the channel dimensions (for the same material) have a significantly higher influence on the thermal efficiency of the PVT panel. It is possible to observe that the smaller the channel is, the higher optical efficiency (η_o) (up to 5.1% better) and the lower heat loss coefficient (a_1) (up to 48.7% lower) compared to the reference case. The reason is that, as the total collector flow-rate was maintained constant in all the cases, the water velocity through smaller channels is higher as well as the convention heat transfer coefficient (which depends on the hydraulic diameter for laminar flows) (h = 1,141 W/(m^2·K) for the best case (3×2 mm) *vs*. h = 171 W/(m^2·K) for the worst case (40×10 mm)), so more heat can be extracted.

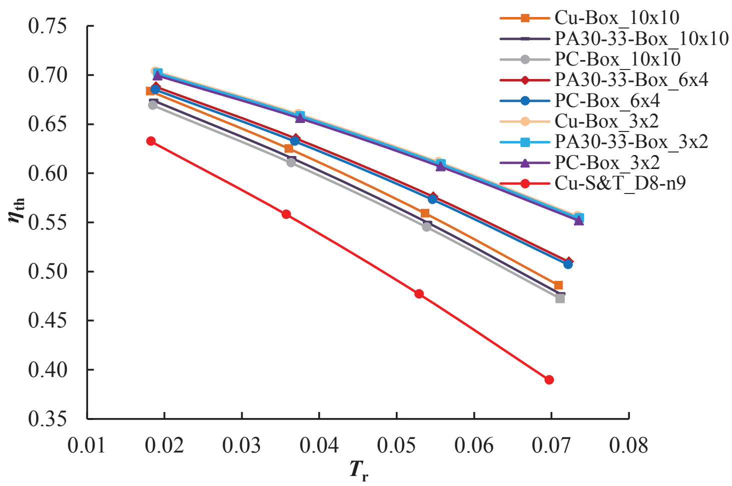

Fig. 6. Performance curves of the most promising PVT configurations studied.

In Figure 6, the most promising PVT configurations studied are presented, which are for channel dimensions of 10×10 mm or lower. These results corroborate that the channel dimensions are determinant in the thermal performance of the PVT panel, while the material does not influence as much. Consequently, it is believed that, in the case of polymeric materials, the higher complexity and costs of loading the polymer with additives might not be outweighed with the increase in thermal performance of the PVT unit. Besides, even though the copper flat-box configuration has the highest thermal performance, the improvement achieved compared to off-the-self polymers (such as Polycarbonate (PC) or Polyamide (PA)) for the same channel dimensions is considerably small. Therefore, a techno-economic analysis is required to bring into consideration other factors such as investment cost and weight to draw conclusions.

4.3 Techno-economic analysis

Table 6 shows a summary of the techno-economic results obtained for the different PVT configurations studied. The heat removal factor (F_R) and the overall heat loss coefficient (U_L) are obtained with Eq. (1), plotting the thermal efficiency (η_{th}) for different water inlet temperatures (T_{in}), and fitting the points to a line (in all fittings, R^2 is higher than 0.997). The results obtained are equivalent to those shown in Figures 5 and 6, with the lowest heat loss coefficient (U_L) and the highest heat removal factors (F_R) in the PVT configurations with smaller channels.

Tab. 6. Summary of the techno-economic results of the different PVT configurations studied.

Configuration	F_R (-)	U_L (W/m^2-K)	T_{PV} (K)	T_{out} (K)	ΔT (K)	w_e (W/m^2)	q_u (W/m^2)	η_e (%)	η_{th} (%)	PBT (days)
Cu-S&T_D8-n9	0.677	-5.739	325.5	336.1	43.1	121.2	632.2	12.1%	63.2%	208
Cu-Box_3x2	0.766	-3.212	318.6	338.3	45.3	125.5	703.6	12.5%	70.4%	236
Cu-Box_10×10	0.738	-4.464	318.3	336.6	43.6	125.7	683.5	12.6%	68.4%	284
Al-Box_10×10	0.743	-4.501	318.3	336.7	43.7	125.6	681.9	12.6%	68.2%	246
Al -Box_20×10	0.744	-4.427	318.7	337.1	44.1	125.4	682.1	12.5%	68.2%	228
PC-Box_3×2	0.761	-3.240	320.3	339.7	46.7	124.4	699.3	12.5%	70.2%	152
PC-Box_6×4	0.748	-3.964	320.6	338.8	45.8	124.2	684.9	12.4%	68.5%	155
PC-Box_10×10	0.729	-4.492	322.5	338.0	45.0	123.1	669.0	12.3%	66.9%	159
PA-Box_10×10	0.722	-4.521	324.2	337.6	44.6	122.0	662.9	12.2%	66.3%	159
PA-Box_20×10	0.723	-4.474	324.2	337.7	44.7	122.0	664.0	12.2%	66.4%	158
PA-Box_40×10	0.711	-4.987	323.7	337.0	44.0	122.3	654.5	12.2%	65.4%	159
PA90-15-Box_10×10	0.731	-4.485	322.0	338.1	45.1	123.3	670.5	12.3%	67.0%	177
PA30-33-Box_3×2	0.764	-3.227	319.4	339.8	46.8	125.0	701.6	12.5%	70.2%	187
PA30-33-Box_6×4	0.751	-3.949	319.6	339.0	46.0	124.8	687.9	12.5%	68.8%	191
PA30-33-Box_10×10	0.734	-4.471	321.1	338.2	45.2	123.9	673.8	12.4%	67.4%	200
PA30-33-Box_20×10	0.734	-4.430	321.5	338.2	45.2	123.7	673.2	12.4%	67.3%	193
PA30-33-Box_40×10	0.721	-4.946	321.4	337.5	44.5	123.7	663.4	12.4%	66.3%	190

The highest average temperature of the PV cells (T_{PV}), and hence the lowest electrical output (w_e) and electrical efficiency (η_e), are obtained for the reference case, which is operating at lower collector flow-rate than the recommended one by the manufacturer, while if it is operated at the nominal flow-rate (0.0083 kg/s (30 L/h)), the PV temperature decreases to 318 K, value lower than for the rest of the configurations. Regarding the flat-box configurations, as expected, the highest PV cell temperatures are reached for the Polyamide (PA) absorber-exchanger, as it has the lowest thermal conductivity (see Table 2). In terms of channel dimensions, the electrical output and electrical efficiency increases as the channel dimensions decreases, as more heat can be extracted (higher useful heat obtained (q_u)) and hence lower PV temperature is reached. On the other hand, it is observed that outlet water temperature (T_{out}) and hence the increment in the water temperature throughout the PVT collector (ΔT) is higher for all flat-box configurations compared to the sheet-and-tube panel, as more heat can be extracted (higher q_u), thanks to the higher heat transfer area of the channels.

Figure 7 shows the total cost savings (€/h) *vs*. the total investment cost (€) of each PVT panel alternative. It is possible to observe that there are two points which differ significantly from the rest (red diamonds) which correspond to the copper flat-box configurations, due to the significantly higher investment cost (as the cost of copper is higher than the aluminium and polymer costs) which is not outweighed by the higher cost savings. Similar results are obtained for the aluminium configurations (green squares). The lowest investment costs are for the polymers without additives, as expected, due to the lower cost of the raw material (dots on the left of the graph), and among them, the best results are obtained for the Polycarbonate (PC) flat-box configuration, in particular the 3×2 mm and 6×4 mm (upper and lower purple triangles respectively) with which high cost savings are achieved, compared to the rest of the channel configurations.

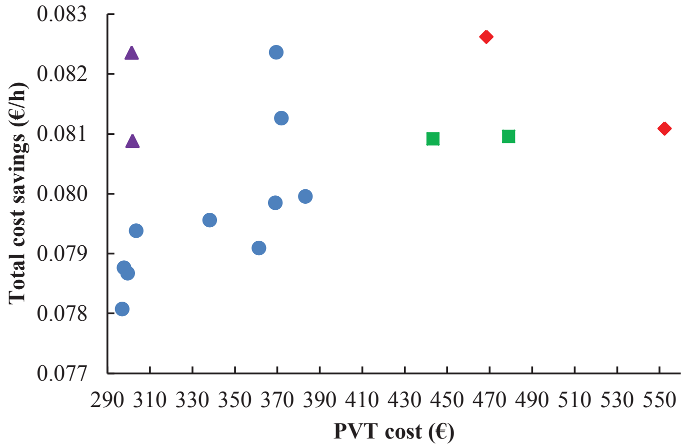

Fig. 7. Total savings (€/h) *vs*. total investment cost of the PVT panel for the different configurations studied. (Red diamonds = copper flat-box, green squares = aluminium flat-box, purple triangles = PC 3×2 mm and 6×4 mm flat-box configurations).

Finally, it is noted that the weight of all polymeric panels can be reduced by 7.5-12%, while the weight of the aluminium flat-box panels increase by 6% and 12% for the 20×10 mm and 10×10 mm configurations, and of the copper flat-box by 48% and 59% for the 3×2 mm and 10×10 mm configurations respectively, compared to the reference case; the absorber-exchanger unit accounts for 17.3% of the total PVT panel weight in the reference sheet-and-tube panel.

5. Conclusions

In this work, 17 different flat-box configurations for the absorber-exchanger unit (plus a benchmark reference case) are applied to the same PVT-w panel in order to compare their performance. The results show that all flat-box configurations have better thermal performance than the copper sheet-and-tube (reference) collector, which is attributed to the larger heat transfer area between the absorber and the fluid in the former configurations. Furthermore, with the flat-box configurations proposed, the temperature distribution on the PV surface is more uniform, avoiding the maximum PV cell temperatures reached between two pipes that appear in the sheet-and-tube collector. As a consequence, although the thermal conductivity of all the polymers considered is lower than the one for copper, all of them achieve a higher optical efficiency (η_o) (up to 5.1% better) and a lower heat loss coefficient (a_1) (up to 48.7% lower) compared to the reference case.

Amongst the different flat-box configurations studied, the results show that for the same channel dimensions, the material does not significantly affect the thermal performance of the PVT collector, with a variation of less than 5% in the performance curves between the best (copper) and worst (Polyamide) configuration. Conversely, the channel dimensions (for the same material) have a significantly higher influence on the thermal efficiency of the PVT panel, varying from around 7% at low water inlet temperatures up to 25% at higher temperatures, between the best (3×2 mm) and worst configuration (40×10 mm). This is attributed to the significantly higher heat transfer coefficient of the water flowing through the channels in the former case (nearly 7 times higher).

Finally, a basic economic consideration of the PVT panels showed that the slightly better thermal performance of the copper and aluminium flat-box configurations do not outweigh their significantly higher investment costs (as the cost of copper and aluminium are higher than the polymer costs). Similarly, among the different polymeric absorber-exchanger alternatives studied, it is observed that the loading of additives considerably increases the investment costs, while only achieving marginal cost savings. Consequently, it can be concluded that the polymeric flat-box configuration is a promising alternative to commercial PVT panels, being able to achieve an improvement in the thermal performance of the PVT unit, while also lowering the investment costs (by up to 22%) and weight (up to 12%) of the PVT panel. However, further work is required to study the thermal expansion of these configurations and its effects on the PV module as well as the performance of the PVT panels under real weather conditions at short and medium term.

Acknowledgement

This work was developed during an international placement of the PhD Candidate Ms. María Herrando at Imperial College London, which was partially funded by University of Zaragoza, Fundación Bancaria Ibercaja and Fundación CAI under the CAI-Ibercaja Program of Research Placements [reference number IT9/16].

References

Agarwal, R.K., Garg, H.P., 1994. Study of a Photovoltaic-Thermal system - Thermosyphonic solar water heater combined with solar cells. Energy Convers. Manag. 35, 605–620.

Allan, J., Dehouche, Z., Stankovic, S., Mauricette, L., 2015. Performance testing of thermal and photovoltaic thermal solar collectors. Energy Sci. Eng. 3, 310–326. doi:10.1002/ese3.75

Antonanzas, J., del Amo, A., Martinez-Gracia, A., Bayod-Rujula, A.A., Antonanzas-Torres, F., 2015. Towards the optimization of convective losses in photovoltaic–thermal panels. Sol. Energy 116, 323–336. doi:10.1016/j.solener.2015.04.013

ASHRAE Standard, 2013. Standard 93-2003 Methods of testing to determine the performance of solar collectors.

Bhattarai, S., Oh, J., Euh, S., Krishna, G., Hyun, D., 2012. Simulation and model validation of sheet and tube type photovoltaic thermal solar system and conventional solar collecting system in transient states. Sol. Energy Mater. Sol. Cells 103, 184–193. doi:10.1016/j.solmat.2012.04.017

Chow, T.T., 2003. Performance analysis of photovoltaic-thermal collector by explicit dynamic model. Sol. Energy 75, 143–152. doi:10.1016/j.solener.2003.07.001

Chow, T.T., He, W., Ji, J., 2006. Hybrid photovoltaic-thermosyphon water heating system for residential application. Sol. Energy 80, 298–306. doi:10.1016/j.solener.2005.02.003

Chow, T.T., Ji, J., He, W., 2007. Photovoltaic-Thermal Collector System for Domestic Application. J. Sol. Energy Eng. 129, 205. doi:10.1115/1.2711474

Collins, M., Zondag, H., 2009. Recommended standard for the characterization and monitoring of PV/Thermal systems, Task 35 - Solar Heating and Cooling Programme (SHC).

Cristofari, C., Canaletti, J., Notton, G., Darras, C., 2012. Innovative patented PV/TH Solar Collector: optimization and performance evaluation. Energy Procedia 14, 235–240.

Cristofari, C., Notton, G., Canaletti, J.L., 2009. Thermal behavior of a copolymer PV/Th solar system in low flow rate conditions. Sol. Energy 83, 1123–1138. doi:10.1016/j.solener.2009.01.008

Cristofari, C., Notton, G., Poggi, P., Louche, A., 2002. Modelling and performance of a copolymer solar water heating collector. Sol. Energy 72, 99–112. doi:10.1016/S0038-092X(01)00092-5

del Amo, A., Martínez-Gracia, A., Bayod-Rújula, A.A., Antoñanzas, J., 2016. An innovative urban energy system constituted by a photovoltaic/thermal hybrid solar installation: Design, simulation and monitoring. Appl. Energy. doi:10.1016/j.apenergy.2016.07.011

EndeF Engineering, 2016. Technical Datasheet ECOMESH panel.

Ghaffari Mosanenzadeh, S., Liu, M.W., Osia, A., Naguib, H.E., 2015. Thermal Composites of Biobased Polyamide with Boron Nitride Micro Networks. J. Polym. Environ. 23, 566–579. doi:10.1007/s10924-015-0733-8

Guarracino, I., Freeman, J., Ekins-daukes, N., Markides, C.N., 2016a. Performance assessment and comparison of solar ORC and hybrid PVT systems for the combined distributed generation of domestic heat and power. International Conference on Heat Transfer, Fluid Mechanics and Thermodynamics.

Guarracino, I., Freeman, J., Markides, C.N., 2016b. Experimental validation of a 3-D dynamic solar- thermal collector model under time-varying environmental conditions. The 29th International Conference On Efficiency, Cost, Optimization, Simulation And Environmental Impact Of Energy Systems.

Guarracino, I., Mellor, A., Ekins-daukes, N.J., Markides, C.N., 2016c. Dynamic coupled thermal-and-electrical modelling of sheet-and-tube hybrid photovoltaic / thermal (PVT) collectors. Appl. Therm. Eng. 101, 778–795. doi: 10.1016/j.applthermaleng.2016.02.056

He, W., Chow, T., Ji, J., Lu, J., Pei, G., 2006. Hybrid photovoltaic and thermal solar-collector designed for natural circulation of water. Appl. Energy 83, 199-210. doi:10.1016/j.apenergy.2005.02.007

Herrando, M., Markides, C.N., 2016. Hybrid PV and solar-thermal systems for domestic heat and power provision in the UK: Techno-economic considerations. Appl. Energy 161, 512–532. doi:10.1016/j.apenergy.2015.09.025

Herrando, M., Markides, C.N., Hellgardt, K., 2014. A UK-based assessment of hybrid PV and solar-thermal systems for domestic heating and power: System performance. Appl. Energy 122, 288–309. doi:10.1016/j.apenergy.2014.01.061

Huang, B.J., Lin, T.H., Hung, W.C., Sun, F.S., 2001. Performance evaluation of solar photovoltaic / thermal systems. Sol. Energy 70, 443–448.

ISO, 2013. ISO 9806:2013 (e) Solar energy - solar thermal collectors - test methods.

Kalogirou, S.A., 2004. Solar thermal collectors and applications. Prog. Ener. Comb. Science 30, 231-295. doi:10.1016/j.pecs.2004.02.001

Kalogirou, S.A., 2001. Use of TRNSYS for modelling and simulation of a hybrid pv–thermal solar system for Cyprus. Renew. Energy 23, 247–260. doi:10.1016/S0960-1481(00)00176-2

Notton, G., Cristofari, C., Mattei, M., Poggi, P., 2005. Modelling of a double-glass photovoltaic module using finite differences. Appl. Therm. Eng. 25, 2854–2877. doi:10.1016/j.applthermaleng.2005.02.008

Sandnes, B., Rekstad, J., 2002. A photovoltaic/thermal (PV/T) collector with a polymer absorber plate. Experimental study and analytical model. Sol. Energy 72, 63–73. doi:10.1016/S0038-092X(01)00091-3

Tiwari, A., Sodha, M.S., 2006. Performance evaluation of solar PV/T system: An experimental validation. Sol. Energy 80, 751–759. doi:10.1016/j.solener.2005.07.006

Tripanagnostopoulos, Y., Souliotis, M., Battisti, R., Corrado, A., 2005. Energy, cost and LCA results of PV and hybrid PV/T solar systems. Prog. Photovoltaics Res. Appl. 13, 235–250. doi:10.1002/pip.590

Vokas, G., Christandonis, N., Skittides, F., 2006. Hybrid photovoltaic – thermal systems for domestic heating and cooling — A theoretical approach. Sol. Energy 80, 607–615. doi:10.1016/j.solener.2005.03.011

Zondag, H.A., de Vries, D.W., van Helden, W.G.J., van Zolingen, R.J.C., van Steenhoven, A.A., 2003. The yield of different combined PV-thermal collector designs. Sol. Energy 74, 253–269. doi:10.1016/S0038-092X(03)00121-X

Zondag, H.A., de Vries, D.W., Van Helden, W.G.J., Van Zolingen, R.J.C., Van Steenhoven, A.A., 2002. The thermal and electrical yield of a PV-thermal collector. Sol. Energy 72, 113–128. doi:10.1016/S0038-092X(01)00094-9